

The effects of water uptake on mechanical properties of viscose fibers

Christian Ganser · Patrice Kreiml · Roland Morak · Frederik Weber · Oskar Paris · Robert Schennach · Christian Teichert

Received: 20 February 2015 / Accepted: 20 May 2015 / Published online: 29 May 2015
© Springer Science+Business Media Dordrecht 2015

Abstract The fact that cellulose materials soften with water uptake is exploited constantly during paper production to form strong bonds between two fibers. Here, we present measurements of surface hardness and reduced modulus of viscose fibers by atomic force microscopy based nanoindentation at varying relative humidity. A home-built setup allowed to access a wide humidity range from 5 % until 95 % relative humidity. The obtained results are compared to those of softwood kraft pulp fibers. Creep effects at a constant load during indentation were observed and found to increase exponentially with increasing humidity. In order to relate mechanical properties to the water content within a fiber, also gravimetric sorption studies were performed. This allowed to extrapolate the mechanical

properties of viscose fibers to 100 % relative humidity. Interestingly, hardness and reduced modulus are at this point higher by a factor of 4 and 20, respectively, compared to those of viscose fibers fully swollen in water. Pulp fibers, in comparison, exhibit mechanical properties which are similar to those of viscose fibers. Only when the fibers are swollen, a higher hardness for viscose fibers is evident, whereas the moduli of pulp and viscose fibers are still comparable.

Keywords Viscose fibers · Pulp fibers · Atomic force microscopy · Nanoindentation · Humidity · Water sorption

C. Ganser · P. Kreiml · F. Weber · R. Schennach · C. Teichert
Christian Doppler Laboratory for Surface Chemical and Physical Fundamentals of Paper Strength, Graz University of Technology, Graz, Austria

C. Ganser (✉) · P. Kreiml · R. Morak · O. Paris · C. Teichert (✉)
Institute of Physics, Montanuniversitaet Leoben, Leoben, Austria
e-mail: christian.ganser@alumni.unileoben.ac.at

C. Teichert
e-mail: teichert@unileoben.ac.at

F. Weber · R. Schennach
Institute of Solid State Physics, Graz University of Technology, Graz, Austria

Introduction

It is long known that cellulose materials swell and soften when placed in water, a feature which is prominently exploited during papermaking. There, a bond between two pulp fibers can form and achieve a high area in molecular contact because the fibers' resistance against mechanical deformation is lowered. Viscose fibers are also reported to be formed into all-viscose paper (Weber et al. 2013, 2014) or used as additives to improve properties of standard paper (Yu et al. 1999). Additionally, viscose fibers can be viewed as model systems for paper fibers, exhibiting a simpler composition and surface as well as bulk structure.

In most applications, cellulose based materials are exposed to an atmosphere with non-constant humidity. Obviously, a change in humidity will result in a change in the water content of cellulose fibers which, in turn, affects their mechanical properties. To test the humidity dependent viscoelastic properties of cellulose fibers or cellulose films, dynamic mechanical analysis (DMA) is often applied (Zhou et al. 2001; Yakimets et al. 2007). There, a complex numbered elastic modulus is detected, with the real part named storage modulus and the imaginary part loss modulus. However, when it is of interest to detect the mechanical properties in terms of the more common Young's modulus and tensile strength, tensile tests are performed (Burgert et al. 2003; Sun et al. 2009).

In particular, nanoindentation (NI) is frequently applied to cellulose fibers, when local properties need to be determined (Gindl et al. 2004, 2006; Lee et al. 2007). To properly use this method, it is essential to prepare smooth sample surfaces. In fact, all NI studies deal with microtome cut longitudinal or radial cross-sections, to provide a smooth and flat sample area.

To obtain mechanical properties of cellulose fibers relevant for bond formation, it would be best to measure them directly at the pristine fiber surface. This is usually not done by NI, since pulp fibers, as well as some viscose fiber types, have rough surfaces. An obvious solution is to first image the surface area and then hand-pick sufficiently flat areas. However, scanning with a nanoindenter can destroy the sample surface, especially in the case of soft samples such as cellulose. To circumvent this problem, atomic force microscopy based NI (AFM-NI) can be applied. There, the surface can be imaged in the gentle tapping mode without damaging it (Zhong et al. 1993). AFM-NI has been commonly applied to polymers (Clifford and Seah 2005; Tranchida et al. 2006; Jee and Lee 2010), and biological matter (Roos and Wuite 2009; Fuhrmann et al. 2011), including pulp fibers (Yan and Li 2013; Ganser et al. 2014a) and viscose fibers (Ganser et al. 2014b).

In this work, we determine the humidity dependent reduced modulus E_r and the hardness H of viscose fibers by AFM-NI and compare them to those of pulp fibers. Furthermore, the water content w of viscose fibers as a function of relative humidity φ_r is detected using a gravimetric sorption system (GSS). This allowed to describe H and E_r also as a function of the fibers' water content.

Methods and materials

Atomic force microscopy based nanoindentation

AFM-NI experiments were performed by employing an Asylum Research MFP-3D AFM (Santa Barbara, CA). The system is equipped with a closed-loop planar sample scanner and has been operated in tapping mode for imaging and in contact mode to collect force-vs.-distance plots. For all experiments, ND-DYIRS full diamond probes (Advanced Diamond Technologies, Romeoville, IL) were used. These probes have a four-sided pyramid as a tip, with an angle of about 75° between two opposite side planes. The radius at the tip apex is less than 50 nm. In the MFP-3D AFM—as with most commercial systems—the probe is tilted by 11°, leading to an asymmetric tip shape.

To study the effects of water uptake on a sample's mechanical properties, a setup to control relative humidity was employed. The used setup is described by Ganser et al. (2014a) and was modified by adding the possibility of heating the buffer segment. This modification allowed to reach relative humidities φ_r within 0.05 and 0.95. The tolerance of the SHT21 humidity sensors (Sensirion AG, Switzerland) is $\Delta\varphi_r = 0.03$ from $\varphi_r = 0.2$ to $\varphi_r = 0.8$ and increases linearly to $\Delta\varphi_r = 0.05$ beyond this interval. To ensure that at a selected value for φ_r an equilibrium in water uptake has been reached, subsequent AFM scans of the fiber under investigation were performed until no drift was observed in the images. Then, the geometrical swelling of the fiber was assumed to be completed (Ganser et al. 2014a).

The detailed procedure of AFM-NI is given by Ganser et al. (2014a), therefore only a brief outline will be presented here. After the collection of force-versus-distance plots, the cantilever's deflection was subtracted from the distance to obtain force-versus-indentation depth plots. These plots were then evaluated according to Oliver and Pharr (1992) with applied modifications for viscoelastic materials (Tang and Ngan 2003). From this procedure, hardness

$$H = \frac{P_{max}}{A(x_c)} \quad (1)$$

and reduced modulus

$$E_r = \frac{\sqrt{\pi}}{2} \frac{S}{\sqrt{A(x_c)}} \quad (2)$$

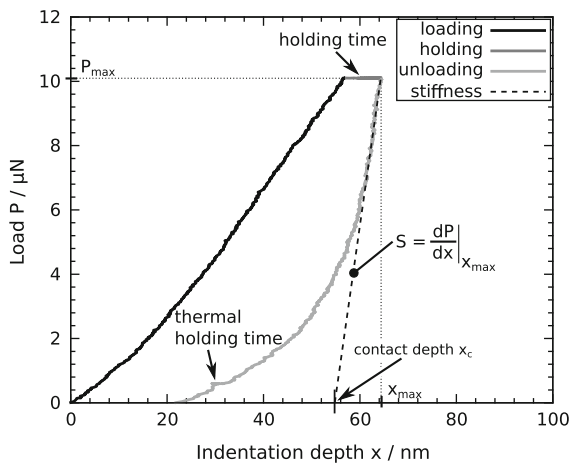


Fig. 1 Exemplary force-versus-indentation depth plot to illustrate the necessary quantities needed to calculate hardness and reduced modulus. This particular curve was recorded on a viscose fiber surface at $\varphi_r \approx 0.05$

are obtained. P_{max} denotes the maximum applied load, $A(x_c)$ the projected area of the tip at the contact depth x_c , and S describes the slope at the beginning of the unloading segment $S = \left. \frac{dP}{dx} \right|_{x_{max}}$. The quantities P_{max} , x_c , and S are illustrated in an exemplary force-vs.-indentation depth plot in Fig. 1.

The hardness obtained by Eq. 1 is related to a material's tensile strength, whereas the reduced modulus (Eq. 2) is linked to the Young's modulus. In principle, the Young's modulus can be calculated from E_r , provided that the material is isotropic. However, this is neither the case for spun fibers nor for natural pulp fibers, therefore, no corrections were applied and E_r is presented as the result.

The load schedule used to collect all force-versus-distance plots had a loading and unloading rate of $10 \mu\text{N s}^{-1}$, a holding time at the maximum load of 10s to compensate for viscoelastic effects, and a holding time of 30 s close to the end of the unloading part at 5 % of the maximum load to allow determination of the thermal drift rate and subsequent correction thereof. In Fig. 1, the effect of the holding time at P_{max} is clearly visible as it leads to an increase in the indentation depth at constant load.

An advantage of AFM-NI over classical NI is that with the AFM's gentle tapping mode, an inspection of the surface before indentation is possible. Although modern nanoindenters also provide a scanning stage, the recording of the surface topography is done in

contact mode, which is known to damage soft surfaces during scanning.

It should be noted that AFM-NI differs from classical NI with respect to the load application. In classical NI, a transducer is used to apply a load perpendicular to the sample's surface. During an AFM-NI experiment, however, the AFM's cantilever bends during load application, thereby slightly tilting the tip with respect to the surface. Therefore, the load is not applied perfectly perpendicular to the surface. Consequently, H and E_r obtained by AFM-NI are not directly comparable to those obtained by NI and a calculation of the Young's modulus from E_r is not straightforward, even if the sample is isotropic.

All viscose fiber samples were classical viscose fibers provided by Kelheim Fibres (Kelheim, Germany). Pulp fibers were bleached softwood kraft pulp fibers. Since the pulp is a mixture of spruce and pine, it is not possible to determine which exact fiber type was investigated. The fibers were placed on a drop of uncured nail polish which was subsequently cured (Schmied et al. 2012; Fischer et al. 2014). This preparation procedure ensures a fixation of the fibers and inhibits their vertical movement during AFM-NI (Ganser et al. 2014a).

Gravimetric sorption

The GSS that was used to measure sorption isotherms is a home-built semiautomatic gas sorption apparatus based on a symmetric two-pan vacuum ultra-microbalance (Sartorius Instruments, model S3D) described elsewhere (Groß and Findenegg 1997). To record an isotherm, gas or vapor is dosed towards the sample until a certain target pressure is reached. After a default equilibration time, the mass uptake of the sample—placed inside a gold coated glass bowl—is recorded. In order to be able to separate the sample's mass increase from the one of the sample bowl, a second bowl is fixed the same way at the other side of the balance's beam. With this, the measured mass increase is no longer influenced by the sample holder. The above described procedure is repeated for selected pressure values of the sorption branch until the saturation pressure is reached. For desorption, the pressure is reduced via a connection with a vacuum pump. In this work, only the sorption is shown, which includes adsorption and absorption. The former denotes the attachment of a substance to an interface,

whereas the latter is used to describe that a substance is incorporated into the bulk of another material. Both, adsorption and absorption, occur in the presented GSS data and are not separated from each other.

To measure the sorption isotherm of viscose fibers, a loose bundle of fibers with a dry mass of 20.6 mg was prepared. The bundle was placed inside a gold coated glass bowl of 10 mm diameter and 6 mm height. The gold coating is hydrophobic and ensures, therefore, that the water will attach preferentially to the sample and not to the bowl.

Results and discussion

Hardness and reduced modulus

As expected, a decrease of hardness and reduced modulus with increasing relative humidity φ_r was observed for classical viscose fibers. This fact becomes already evident when comparing the residual indents on viscose fiber surfaces, presented in Fig. 2. The AFM topography images in Fig. 2a show that the residual indents become larger at higher humidities. At $\varphi_r = 0.10$, the indents have a side length of approximately 150 nm while at $\varphi_r = 0.94$ the side length is about 400 nm. The line profiles in Fig. 2b also indicate an increase in the persistent indentation depth from about 30 nm at $\varphi_r = 0.10$ to about 50 nm at $\varphi_r = 0.94$.

It is already apparent from Fig. 2 that at low humidities pile-ups occur at the left and right sides of the indents. This is visualized more clearly in Fig. 3.

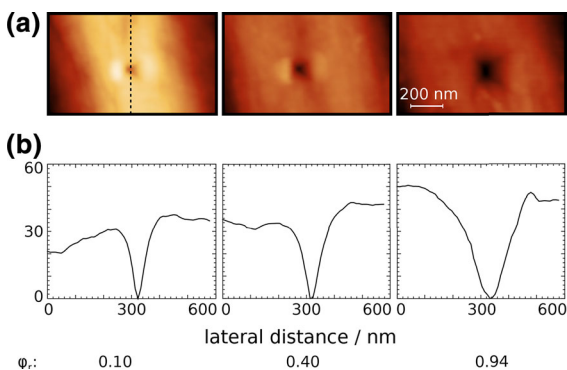


Fig. 2 Indents on viscose fibers at different humidities. **a** $1.0 \mu\text{m} \times 0.6 \mu\text{m}$ AFM topography images. **b** Line profiles in vertical direction, indicated by the dotted line in (a)

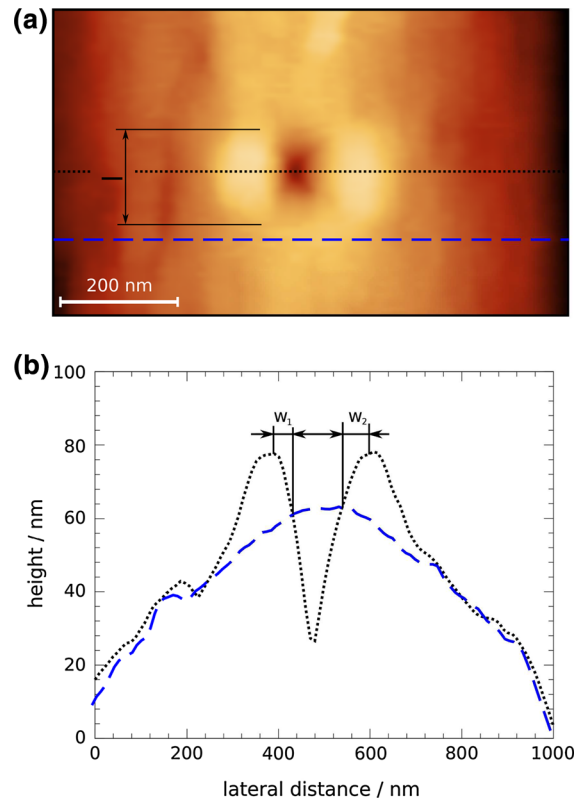


Fig. 3 The occurrence of the pile-up effect on a viscose fiber **(a)** illustrated by a $10 \mu\text{m} \times 6 \mu\text{m}$ AFM topography image and **(b)** two line profiles to demonstrate its extent. w_1 and w_2 describe the width of the pile-up and l its length. The dotted line and the dashed line in (a) mark the position of the respective line profile in (b)

In Fig. 3a, the topography is presented and in Fig. 3b line profiles at the positions indicated in Fig. 3a are plotted. These profiles clearly reveal that a severe pile-up of material at the left and right sides of an indent is present. Since the cantilever is oriented horizontally by performing the indent in Fig. 3a, the pile-up could be caused by the lateral force component due to the bending of the cantilever in AFM-NI. On the other hand, the fiber's longitudinal axis was oriented perpendicular to the cantilever, i.e., vertically in Fig. 3a. Since viscose fibers are anisotropic, this could also explain a pile-up only on two sides. By rotating the fiber with respect to the cantilever and performing indents, a pile-up on three sides was found. One pile-up was caused by the bending of the cantilever and the other two pile-ups by the anisotropy, as they were similar to those in Fig. 3a. Therefore, we believe that the pile-ups visible in Figs. 2 and 3 stem from the

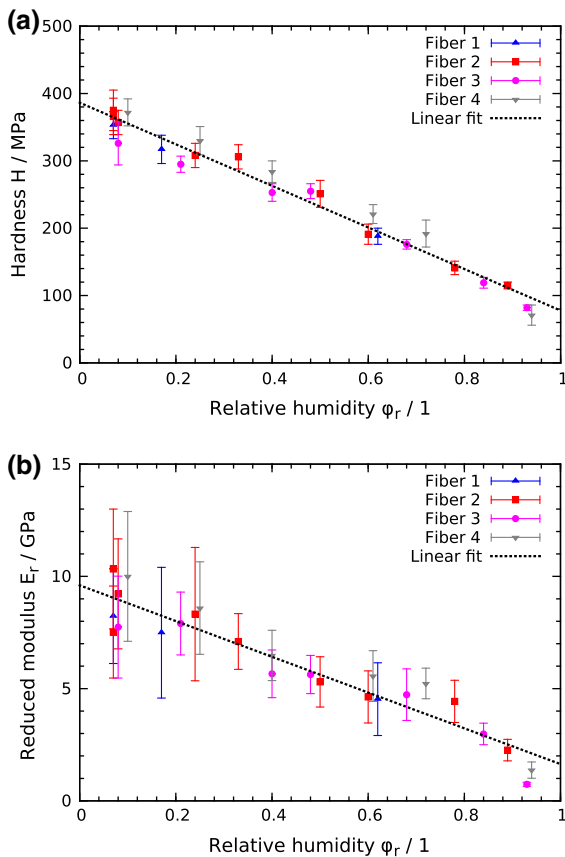


Fig. 4 The dependence of mechanical properties of viscose fibers on relative humidity. **a** Hardness and **b** reduced modulus. The *dotted line* represents a linear fit

fibers' anisotropy as well as from the bending of the cantilever during AFM-NI.

The consequence of such a pile-up of material is that it increases the contact area during indentation and hence leads to an overestimation of H and E_r . Because of this fact, it is necessary to correct the H and E_r values obtained by the method of Oliver and Pharr for the pile-up. This correction was performed according to Kese et al. (2005) by measuring the widths w_1 and w_2 and length l of the pile-ups and approximating the additional area by a semi-ellipse. All indents performed at relative humidities below 0.9 were corrected. Above this value of ϕ_r , no pile-up was observed.

The evolution of the corrected mechanical properties of classical viscose fibers with relative humidity is plotted in Fig. 4. The hardness (Fig. 4a) as well as the reduced modulus (Fig. 4b) exhibit an approximately

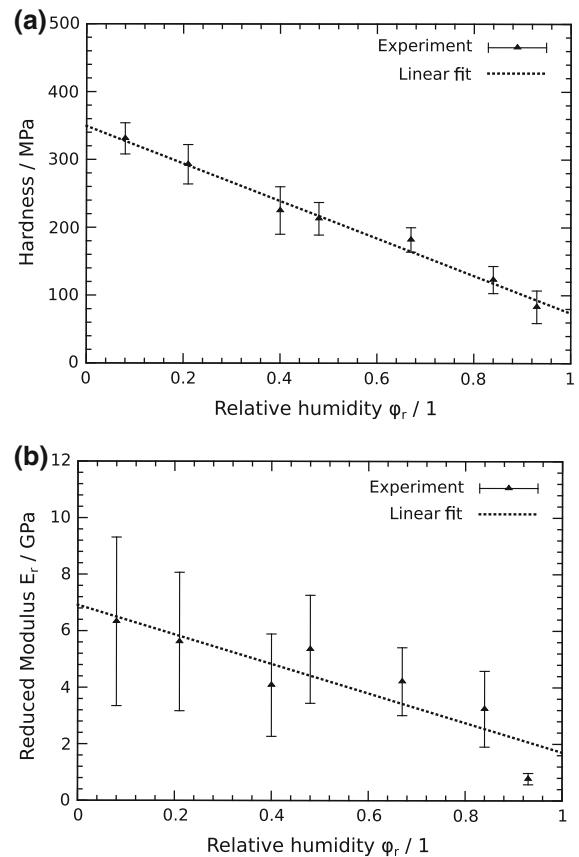


Fig. 5 The dependence of mechanical properties of kraft pulp fibers on relative humidity. **a** Hardness and **b** reduced modulus

linear decrease with increasing relative humidity. The reduced modulus, however, seems to feature a kink at $\phi_r \approx 0.75$ after which a stronger decrease is observed. A definite identification of a kink is hindered by the large standard deviation in E_r , and a linear decrease is equally likely from the present data. For hardness H , the data points at $\phi_r \approx 0.95$ deviate slightly from a linear trend, but not significantly.

In the literature, such a kink in the elastic modulus has been reported (Zhou et al. 2001). There, the elastic modulus of regenerated cellulose films was determined by DMA as a function of relative humidity, and the storage modulus as well as the loss modulus were reported to exhibit a kink at $\phi_r \approx 0.80$.

As a comparison, the change of a kraft pulp fiber's mechanical properties with relative humidity is presented in Fig. 5. These values were determined simultaneously as those of the classical viscose fiber number 3 presented in Fig. 4. It was achieved by

Table 1 Hardness and reduced modulus of fully swollen fibers in water, including values for viscose fibers at $\varphi_r = 1.0$, predicted by Eq. 8

Material	H/MPa	E_r/GPa	No. of indents
Viscose [†]	14 ± 1.0	0.051 ± 0.011	37
Pulp	6.9 ± 2.8	0.046 ± 0.017	88
Prediction by Eq. 8 (viscose)	51	1.1	—

[†] From Ganser et al. (2014b)

gluing a pulp fiber next to a viscose fiber and recording force distance curves in an alternating manner. Hardness of a kraft pulp fiber, plotted in Fig. 5a, and reduced modulus (Fig. 5b) exhibit a similar behavior as classical viscose fibers on increasing humidity. It is not possible to decide whether a kink in E_r is present or not because only seven data points on one pulp fiber were recorded. For classical viscose fibers, on the other hand, 25 data points were obtained on four different fibers. But it is obvious that the measured E_r of pulp fibers at $\varphi_r \approx 0.95$ is decreased more than what is predicted by a linear relationship between E_r and φ_r .

When a fiber is immersed in water and swollen for several hours, H and E_r of fully swollen fibers in the wet state are obtained. The results of such experiments are given in Table 1. These values are not plotted in Figs. 4 and 5, because they were obtained by providing liquid water for swelling, which is in contrast to all other values presented in these figures. Also, these wet-state values are so small that in Figs. 4 and 5 they would appear to be 0.

With these data, all states of humid cellulose fibers were sampled and a comparison between pulp and viscose is possible. While the hardness H in humid nitrogen is basically the same for pulp fibers as well as for viscose fibers, the reduced modulus E_r seems higher for viscose fibers. To investigate this in more detail, the ratios of hardness and reduced modulus between viscose and pulp fibers, i.e.

$$r_H = \frac{H_v}{H_p} \tag{3}$$

and

$$r_E = \frac{E_{r,v}}{E_{r,p}} \tag{4}$$

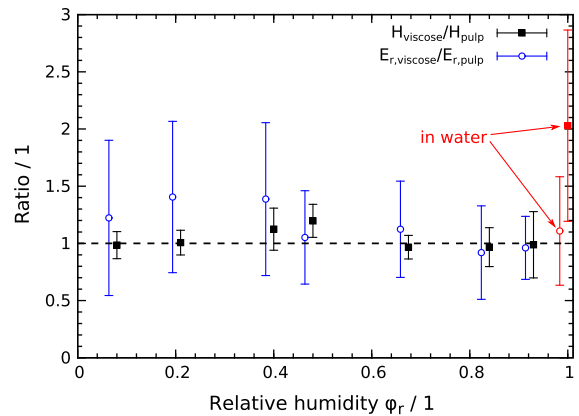


Fig. 6 Comparison of H and E_r of viscose and pulp fibers by the ratios r_H (filled squares) and r_E (open circles). The relative humidity values are the same for both ratios but the modulus ratios were shifted to the left by $\Delta\varphi_r = 0.015$ for clarity's sake. The dashed line indicates a ratio of 1. The two rightmost data points were obtained from fibers swollen in water

are plotted in Fig. 6 as a function of φ_r . The indices v and p denote a quantity which is obtained from viscose or pulp fibers, respectively. The error bars were calculated from the individual standard deviations by employing error propagation. Considering only the values obtained in humid nitrogen atmosphere, r_H is mostly close to unity, whereas r_E reaches values between 1.2 and 1.5 from $\varphi_r = 0$ until $\varphi_r = 0.5$ and is then also approximately constant at 1. Due to the large errors, however, one can assume that E_r is also the same for both materials.

When pulp and viscose fibers were immersed in water and swollen for several hours, it appears that the reduced modulus is still similar for both materials ($r_E \approx 1$). However, the hardness in water is higher for viscose fibers than for pulp fibers with $r_H \approx 2$ in this state, as it is visible in Fig. 6. According to a Welch test (Welch 1947) at a significance level of 0.01, there is a significant difference in hardness between fully swollen pulp and viscose fibers. Their moduli, however, do not differ significantly. Both observations are in accordance to earlier findings (Ganser et al. 2014b).

Creep effects

Due to the fact that the $P - x$ plots are recorded with a hold time of 10 s at P_{max} , it is straightforward to extract also a measure for the creep effect. This is the distance which the indenter sinks into the material at

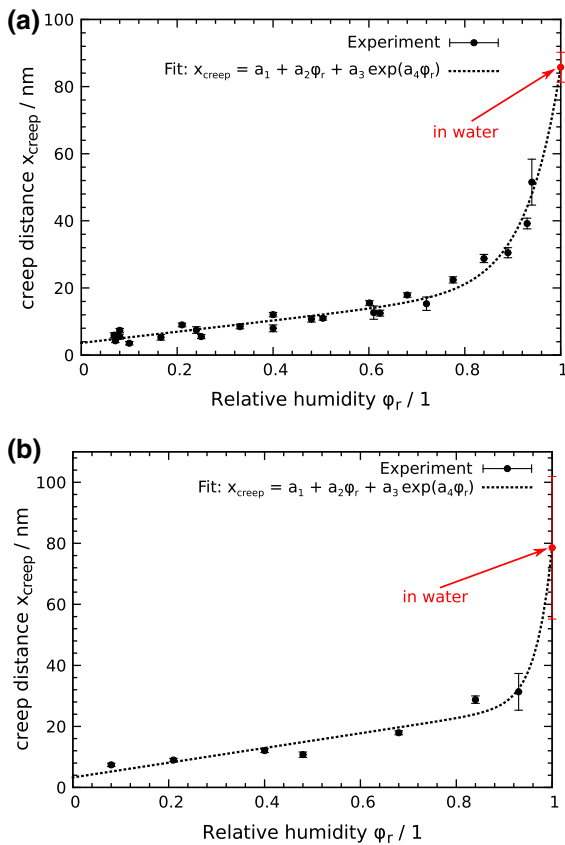


Fig. 7 Increase in indentation depth at maximum load as a function of relative humidity for (a) classical viscose and (b) a pulp fiber

constant load, as is evident from Fig. 1. The creep distance x_{creep} is plotted against the relative humidity in Fig. 7a, b for viscose fibers and pulp fibers, respectively. It is not surprising that x_{creep} is increasing with increasing humidity. The creep distance for viscose seems to be well described by the relation

$$x_{creep}(\varphi_r) = a_1 + a_2\varphi_r + a_3 \exp(a_4\varphi_r), \tag{5}$$

which has been found by us empirically. Equation 5 fits best the data obtained on viscose fibers. While x_{creep} measured on the pulp fiber seems also likely to follow Eq. 5, its validity for this case is less certain due to a lack of data points, compared to viscose fibers. Apparently, until $\varphi_r \approx 0.7$, the increase in creep distance is mostly linear. Only for $\varphi_r > 0.7$, the exponential part kicks in and x_{creep} increases stronger than linear. Note that the creep distance of fully swollen viscose fibers in water lies on the same curve as the ones measured in humid air. This suggests that

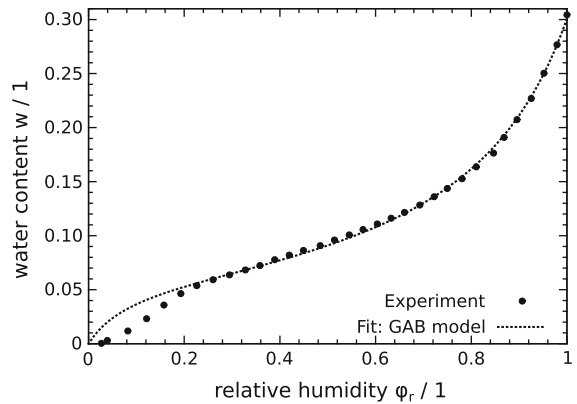


Fig. 8 Sorption isotherm of viscose fibers at a temperature of 17 °C. Filled circles GSS experiment, dotted line fit with the GAB model

there is no or little difference in viscoelastic properties between viscose fibers in humid air at $\varphi_r = 1$ and fully swollen viscose fibers in water. It is unclear if this holds also for pulp fibers. For the pulp fiber, the kink is located at $\varphi_r \approx 0.9$ and is clearly induced by the high value of x_{creep} measured in water.

Water uptake

The reason why viscose fibers become softer with increasing relative humidity is that water from the environment is absorbed by the material’s bulk. There, water will weaken the hydrogen bonds which are the dominant bond type within the material. It is therefore of interest to convert the relative humidity φ_r to the water content, defined as

$$w = \frac{m_{H_2O}}{m_{viscose}}. \tag{6}$$

m_{H_2O} denotes the mass of the sorbed water by the viscose and $m_{viscose}$ the viscose fibers’ dry mass. With the AFM setup outlined in Sect. 2.1, only φ_r can be detected, but not w , therefore a GSS is used which allows the measurement of a material’s mass increase as a function of the water vapor pressure—and hence φ_r . This setup has been described in Sect. 2.2. The sorption isotherm of the same type of viscose fibers characterized with AFM-NI is presented in Fig. 8. To allow the transformation of φ_r to w , the isotherm was fitted with the Guggenheim–Anderson–de Boer (GAB) model (Anderson 1946; de Boer 1953; Guggenheim 1966), which is frequently used to describe sorption isotherms of various materials,

including cellulose (Delwiche et al. 1991; Belbekhouche et al. 2011; Sun 2008). The GAB model describes $w(\varphi_r)$ as

$$w(\varphi_r) = \frac{AB\varphi_r}{(1 - B\varphi_r)(1 - B\varphi_r + AB\varphi_r)}. \tag{7}$$

A is the sorption constant as is appears in the Brunauer–Emmett–Teller (BET) isotherm (Brunauer et al. 1938) and B accounts for the fact that the heat of adsorption for the layers two to nine is less than those following these (Anderson 1946; Delwiche et al. 1991).

GSS measurements with our setup required a mass of about 20 mg, which corresponds to a number of approximately 4000 single fibers (5 mm fiber length, 30 μm fiber diameter, 1500 kg/m^3 cellulose density) or a total fiber length of almost 20 m. Although effects attributed to the fiber network (such as capillary condensation at fiber-fiber crossings) are present in this approach, we believe them to be negligible. The water content obtained by GSS is, therefore, considered as a good estimate for the water content in a single fiber.

It is obvious from Fig. 8 that the experimentally obtained data points follow the GAB model only for $\varphi > 0.2$. Thus, the fit with Eq. 7 was performed within the interval $0.2 \leq \varphi_r \leq 1.0$. This will affect only the transformation of the H and E_r values obtained at the lowest humidities at around $\varphi_r = 0.05$ to 0.15, which are bunched together at the very left in Fig. 4.

The plot of hardness and reduced modulus as a function of the water content w is shown in Fig. 9a, b, respectively. Apparently, the assumption of a linear dependence on w is not appropriate, since it will lead to negative values for H and E_r at $w = 0.304$ (which corresponds to $\varphi_r = 1$). A description of the Young’s modulus E as a function of w for hydrogen bond dominated solids was given by Nissan (1976). There, the decrease of E was considered to be caused by the dissociation of hydrogen bonds due to water infiltrating the material. This yielded the exponential relation

$$\frac{E(w)}{E_0} = \exp(a - bw). \tag{8}$$

E_0 denotes the Young’s modulus at zero water content and is usually determined by fitting data in the interval $0 \leq w \leq w_c$ with $E/E_0 = \exp(-w)$, w_c is postulated to be equal to the BET monolayer and $w_c \approx 0.05$. Then, a

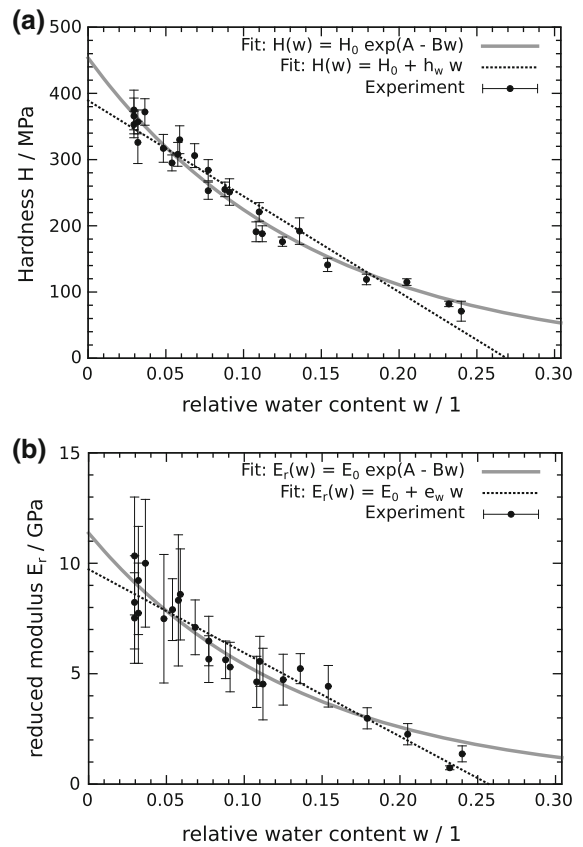


Fig. 9 Hardness (a) and reduced modulus (b) of viscose fibers as a function of the water uptake. The water content w was determined from Fig. 8

and b depend only on w_c , the hypothetical quantity of water needed to provide one water molecule for each OH group of the cellulose molecule, and the average number of hydrogen bonds that will break cooperatively (Nissan 1976). However, our collected data of H and E_r for $0 \leq w \leq w_c$ is insufficient to determine E_0 accurately. Therefore, only the plausibility of Eq. 8 for high water content is checked. Least squares fits of $H(w)$ and $E_r(w)$ with Eq. 8 are presented in Fig. 9. The reduced modulus follows Eq. 8 as expected, even though a large scattering in E_r is present (see Fig. 9b). The change in hardness due to the uptake of water from humid air is also well described by Eq. 8 (Fig. 9a), which was derived initially only for the modulus. However, hardness and modulus do have a relationship, as can be seen by comparing Fig. 4a, b, where H and E_r decrease both with increasing φ_r . In any case, it is obvious that the exponential relation is in

both cases more plausible than a linear relation, when the predicted values for $w = 0.304$ are considered.

It is now interesting to compare values of H and E_r predicted for $w = 0.304$ by Eq. 8 with values measured on fully swollen fibers in water. The model developed by Nissan (1976) does only take into account the uptake of water into cellulose from humid air and cannot be applied when bulk water is present. Using Eq. 8, hardness and reduced modulus at $\varphi_r = 1$ are predicted as $H(w)|_{0.304} = 51$ MPa and $E_r(w)|_{0.304} = 1.1$ GPa. These values are clearly different from the wet-state values presented in Table 1. This means that viscose fibers in humid air will never reach H and E_r values as low as those of fibers swollen in water. A possible explanation for this behavior is that at $\varphi_r = 1$ not all pores or interfibril spaces are filled with water. Only when the viscose fibers are swollen in liquid water, all spaces within the fiber are infiltrated by water and thus the fibers' structure is weakened as much as possible, leading to the lowest values of hardness and reduced modulus. Compared to humid atmosphere at $\varphi_r = 1$, the viscose fibers' hardness is decreased by a factor of almost 4 and the reduced modulus by a factor of about 20 when swelling them for several hours in water. This suggests that viscose fibers still retain a high E_r and a relatively high H , even when swelling them at humidities close to $\varphi_r = 1$. Only the exposure to liquid water will reduce the fibers' resistance against deformation to a minimum. Such a highly weakened state is desirable in, e.g., papermaking where soft swollen fibers will lead to the formation of strong interfiber bonds (Persson et al. 2013).

Conclusions

In this work, we have detected hardness H and reduced modulus E_r of viscose fiber surfaces as a function of the surrounding relative humidity φ_r by AFM-NI. The results obtained on viscose fibers were compared to those of pulp fibers, which appear to have very similar mechanical properties at all humidities. A significant difference between the hardness of viscose and pulp was found only for fully swollen fibers in water, which is consistent with earlier results (Ganser et al. 2014b). Additionally, an exponentially increasing creep distance was found for increasing relative humidity. By

measuring the viscose fibers' water uptake as a function of φ_r with a GSS, the decrease in H and E_r could be related to the fibers' water content w . There, a model based on hydrogen bond dissociation by water (Nissan 1976) was applied and allowed for extrapolating H and E_r to $\varphi_r = 1$. Apparently, only a small decrease of H and E_r takes place between $\varphi_r = 0.95$ and $\varphi_r = 1$ and the materials still retain a relatively high resistance against deformation. In other words, it is substantial that cellulose is swollen in liquid water in order to reach maximum deformability. Such a low resistance against deformation is mandatory in papermaking where it leads to strong interfiber bonds (Persson et al. 2013). A maximum in creep effects, however, might already be reached at $\varphi_r \approx 1$.

Acknowledgments The financial support of the Austrian Federal Ministry of Economy, Family and Youth and the National Foundation for Research, Technology and Development is gratefully acknowledged. We would like to thank Ingo Bernt and Walter Roggenstein (Kelheim Fibres GmbH, Germany) as well as Franz J. Schmied and Leo Arpa (Mondi, Austria) for providing samples and for discussions. We thank Herbert Wormeester and Arzu Colak (University of Twente, Enschede, The Netherlands) for sharing their know-how regarding a controlled humidity setup in AFM.

References

- Anderson RB (1946) Modifications of the Brunauer, Emmett and Teller equation. *J Am Chem Soc* 68(4):686–691
- Belbekhouche S, Bras J, Siqueira G, Chappey C, Lebrun L, Khelifi B, Marais S, Dufresne A (2011) Water sorption behavior and gas barrier properties of cellulose whiskers and microfibrils films. *Carbohydr Polym* 83(4):1740–1748
- Brunauer S, Emmett PH, Teller E (1938) Adsorption of gases in multimolecular layers. *J Am Chem Soc* 60(2):309–319
- Burgert I, Frühmann K, Keckes J, Fratzl P, Stanzl-Tschegg SE (2003) Microtensile testing of wood fibers combined with video extensometry for efficient strain detection. *Holzforchung* 57(6):661–664
- Clifford CA, Seah MP (2005) Quantification issues in the identification of nanoscale regions of homopolymers using modulus measurement via AFM nanoindentation. *Appl Surf Sci* 252(5):1915–1933
- de Boer JH (1953) The dynamical character of adsorption. Clarendon Press, Oxford
- Delwiche SR, Pitt RE, Norris KH (1991) Examination of starch-water and cellulose-water interactions with near infrared (NIR) diffuse reflectance spectroscopy. *Starch-Stärke* 43(11):415–422
- Fischer WJ, Zankel A, Ganser C, Schmied FJ, Schroettner H, Hirn U, Teichert C, Bauer W, Schennach R (2014) Imaging of the formerly bonded area of individual fibre to fibre joints with SEM and AFM. *Cellulose* 21(1):251–260

- Fuhrmann A, Staunton J, Nandakumar V, Banyai N, Davies P, Ros R (2011) AFM stiffness nanotomography of normal, metaplastic and dysplastic human esophageal cells. *Phys Biol* 8(1):015,007
- Ganser C, Hirn U, Rohm S, Schennach R, Teichert C (2014a) AFM nanoindentation of pulp fibers and thin cellulose films at varying relative humidity. *Holzforschung* 68:53–60
- Ganser C, Weber F, Czibula C, Bernt I, Schennach R, Teichert C (2014b) Tuning hardness of swollen viscose fibers. *Bioinspir Biomim Nanobiomater* 3(3):131–138
- Gindl W, Gupta H, Schöberl T, Lichtenegger H, Fratzl P (2004) Mechanical properties of spruce wood cell walls by nanoindentation. *Appl Phys A Mater* 79(8):2069–2073
- Gindl W, Konnerth J, Schöberl T (2006) Nanoindentation of regenerated cellulose fibres. *Cellulose* 13:1–7
- Groß S, Findenegg GH (1997) Pore condensation in novel highly ordered mesoporous silica. *Ber Bunsen Ges Phys Chem* 101(11):1726–1730
- Guggenheim EA (1966) Application of statistical mechanics. Clarendon Press, Oxford
- Jee AY, Lee M (2010) Comparative analysis on the nanoindentation of polymers using atomic force microscopy. *Polym Test* 29(1):95–99
- Kese K, Li ZC, Bergman B (2005) Method to account for true contact area in soda-lime glass during nanoindentation with the Berkovich tip. *Mater Sci Eng A Struct* 404:1–8
- Lee SH, Wang S, Pharr GM, Kant M, Penumadu D (2007) Mechanical properties and creep behavior of lyocell fibers by nanoindentation and nano-tensile testing. *Holzforschung* 61(3):254–260
- Nissan AH (1976) H-bond dissociation in hydrogen bond dominated solids. *Macromolecules* 9(5):840–850
- Oliver W, Pharr G (1992) Improved technique for determining hardness and elastic modulus using load and displacement sensing indentation experiments. *J Mater Res* 7:1564–1583
- Persson BNJ, Ganser C, Schmied F, Teichert C, Schennach R, Gilli E, Hirn U (2013) Adhesion of cellulose fibers in paper. *J Phys Condens Matter* 25(4):045,002
- Roos W, Wuite G (2009) Nanoindentation studies reveal material properties of viruses. *Adv Mater* 21(10–11):1187–1192
- Schmied FJ, Teichert C, Kappel L, Hirn U, Schennach R (2012) Joint strength measurements of individual fiber-fiber bonds: An atomic force microscopy based method. *Rev Sci Instrum* 83(7):073,902–073,902-8. doi:[10.1063/1.4731010](https://doi.org/10.1063/1.4731010)
- Sun CC (2008) Mechanism of moisture induced variations in true density and compaction properties of microcrystalline cellulose. *Int J Pharm* 346(1):93–101
- Sun S, Mitchell JR, MacNaughtan W, Foster TJ, Harabagiu V, Song Y, Zheng Q (2009) Comparison of the mechanical properties of cellulose and starch films. *Biomacromolecules* 11(1):126–132
- Tang B, Ngan AHW (2003) Accurate measurement of tipsample contact size during nanoindentation of viscoelastic materials. *J Mater Res* 18:1141–1148
- Tranchida D, Piccarolo S, Soliman M (2006) Nanoscale Mechanical Characterization of Polymers by AFM Nanoindentations: Critical Approach to the Elastic Characterization. *Macromolecules* 39(13):4547–4556
- Weber F, Koller G, Schennach R, Bernt I, Eckhart R (2013) The surface charge of regenerated cellulose fibres. *Cellulose* 20(6):2719–2729
- Weber F, Ganser C, Teichert C, Schennach R, Bernt I, Eckhart R (2014) Application of the Page-equation on flat shaped viscose fibre handsheets. *Cellulose* 21(5):3715–3724
- Welch B (1947) The generalization of student's problem when several different population variances are involved. *Biometrika* 34:28–35
- Yakimets I, Paes SS, Wellner N, Smith AC, Wilson RH, Mitchell JR (2007) Effect of water content on the structural reorganization and elastic properties of biopolymer films: a comparative study. *Biomacromolecules* 8(5):1710–1722
- Yan D, Li K (2013) Conformability of wood fiber surface determined by AFM indentation. *J Mater Sci* 48:322–331
- Yu Y, Kettunen H, Niskanen K (1999) Can viscose fibres reinforce paper? *J Pulp Pap Sci* 25(11):398–402
- Zhong Q, Inniss D, Kjoller K, Elings V (1993) Fractured polymer/silica fiber surface studied by tapping mode atomic force microscopy. *Surf Sci Lett* 290(1–2):L688–L692
- Zhou S, Tashiro K, Hongo T, Shirataki H, Yamane C, Ii T (2001) Influence of water on structure and mechanical properties of regenerated cellulose studied by an organized combination of infrared spectra, X-ray diffraction, and dynamic viscoelastic data measured as functions of temperature and humidity. *Macromolecules* 34:1274–1280